Inorganic Graphene Analogues

DOI: 10.1002/anie.201105364

# A Mixed-Solvent Strategy for Efficient Exfoliation of Inorganic Graphene Analogues**

*Kai-Ge Zhou, Nan-Nan Mao, Hang-Xing Wang, Yong Peng, and Hao-Li Zhang**

Layered two-dimensional (2D) nanomaterials such as graphene are a conceptually new class of materials that offers new access to low-dimensional physics.[1–4] Besides well-known graphene, inorganic graphene analogues (IGAs)[5] such as layered transition metal dichalcogenides (e.g., $MoS_2$ and $WS_2$)[5–7] and boron nitride (BN)[8] have been attracting rapidly increasing attention in the past few years. These IGAs were expected to exhibit unique properties and have great potential in applications like transistors,[9–11] energy storage,[12,13] thermal conductors,[14] and topological insulators.[15] Moreover, IGAs like $MoS_2$ and $WS_2$ have intrinsic band gap and high mobility, and may even compete with graphene in certain fields.[9] However, investigations on IGAs have been significantly hindered by the practical difficulties in the preparation and assembly of these 2D nanomaterials.

Only a few approaches to obtain few-layered IGAs have been reported. Mechanical exfoliation[1,16] was first used to obtain layered IGAs from their bulk materials.[9,17] Other approaches that are being explored include chemical synthesis[6,18,19] and liquid exfoliation.[5] Coleman et al. recently reported a surfactant-free liquid-exfoliation method which can produce few-layered nanosheets of IGAs dispersed in various organic solvents.[5] Thermodynamic analysis suggested that, because of the high surface energy of IGAs, the best solvents are likely to have high boiling points.[20,21] Using nonvolatile solvents makes it difficult to process IGAs into devices,[21,22] due to the difficulties in the removal of solvent and the occurrence of aggregation during the slow solvent evaporation. To date, liquid exfoliation of layered $MoS_2$ and $WS_2$ in volatile solvent has met with very limited success.

Herein we demonstrate a versatile and scaleable mixed-solvent strategy for liquid exfoliation of IGAs, including $WS_2$, $MoS_2$, and BN, in volatile solvents. By choosing solvents with appropriate composition, highly stable IGA suspensions can be obtained in low-boiling solvent mixtures, which can then be easily used in further applications.

The dispersion of nanomaterials in liquids can be partially predicted by the theory of Hansen solubility parameters (HSP),[5,23,24] which is a semi-empirical correlation developed to explain dissolution behavior.[23] Three HSP parameters are used to describe the character of a solvent or material: $\delta_D$, $\delta_P$, and $\delta_H$, which are the dispersive, polar, and hydrogen-bonding solubility parameters, respectively. The dissolution process is one of adaptation between the HSP parameters of solvents and solutes. The HSP distance $R_a$ is used to evaluate the level of adaptation [Eq. (1)].

$$R_a = [4(\delta_{D,solv}-\delta_{D,solu})^2 + (\delta_{P,solv}-\delta_{P,solu})^2 + (\delta_{H,solv}-\delta_{H,solu})^2]^{0.5} \quad (1)$$

The smaller the $R_a$ value, the higher the expected solubility. If the HSP parameters of a nanomaterial are known, the $R_a$ value can be used as a guide for finding a single efficient solvent for its dispersion.

Besides single-component solvents, HSP theory can be also applied to solvent mixtures, in which each of the three HSP parameters for a solvent mixture is a linear function of composition [Eq. (2)]

$$\delta_{blend} = \sum \phi_{n,comp}\delta_{n,comp} \quad (2)$$

where $\phi$ is the volume fraction for each composition. Therefore, Equations (1) and (2) enable us to predict the solubility of different nanomaterials in various solvent mixtures, which effectively allows us to design ideal solvent systems. Herein, as a proof of concept, we demonstrate how two "poor" solvents, ethanol and water, can be designed to give high solubility to various IGAs. More details on the calculations of $R_a$ values between different solvent mixtures and IGA materials are given in the Supporting Information.

Figure 1 shows photographs of suspensions containing $MoS_2$, $WS_2$, and BN nanomaterials in different ethanol/water mixtures. Pure ethanol and pure water can hardly disperse any IGAs, but the IGAs exhibit significantly different dispersion properties in ethanol/water mixtures with different compositions. At an appropriate ethanol/water ratio, dark green dispersions of $MoS_2$ and $WS_2$ (Figure 1a and b) and a "milky" BN dispersion (Figure 1c) were obtained, that is, high concentrations of $MoS_2$, $WS_2$, and BN nanomaterials can be successfully dispersed in the mixtures of two poor solvents. These suspensions were highly stable, and showed no precipitation after being stored for a week under ambient conditions.

[*] K.-G. Zhou, N.-N. Mao, H.-X. Wang, Prof. H.-L. Zhang
State Key Laboratory of Applied Organic Chemistry, College of Chemistry and Chemical Engineering, Lanzhou University
Lanzhou 730000 (P. R. China)
E-mail: haoli.zhang@lzu.edu.cn
Homepage: http://sklaoc.lzu.edu.cn/faculty/zhanghl/
Prof. Y. Peng
School of Physical Science and Technology, Lanzhou University
Lanzhou 730000 (P. R. China)

[**] This work is supported by National Natural Science Foundation of China (NSFC. 21073079, J1010067), the Fundamental Research Funds for the Central Universities National Basic Research Program of China (973 Program) No.2012CB933100 and 111 Project. Helps from Mr. Xin-Hua Li in the HRTEM characterizations is also acknowledged.

Supporting information for this article is available on the WWW under http://dx.doi.org/10.1002/anie.201105364.

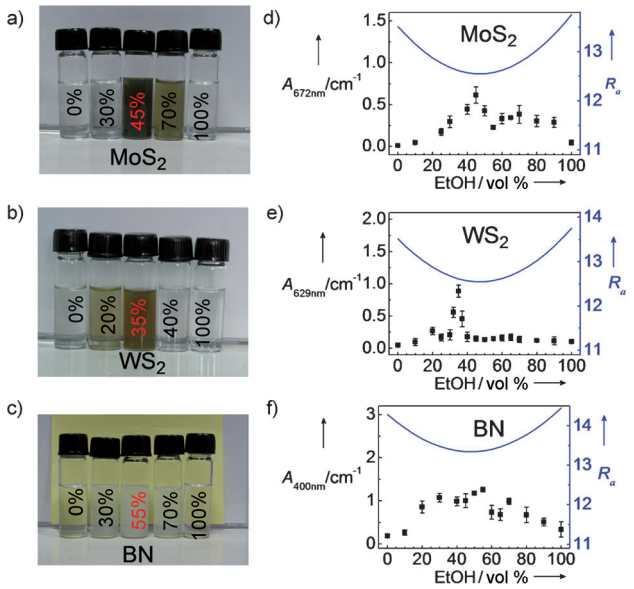


***Figure 1.*** Photographs of a) $MoS_2$, b) $WS_2$, and c) BN dispersions in various ethanol/water mixtures, which have been stored under ambient conditions for a week. The absorbance of the $MoS_2$, $WS_2$, and BN suspensions in ethanol/water mixtures with different composition are shown as dots, and the calculated $R_a$ values as solid lines, in d–f).

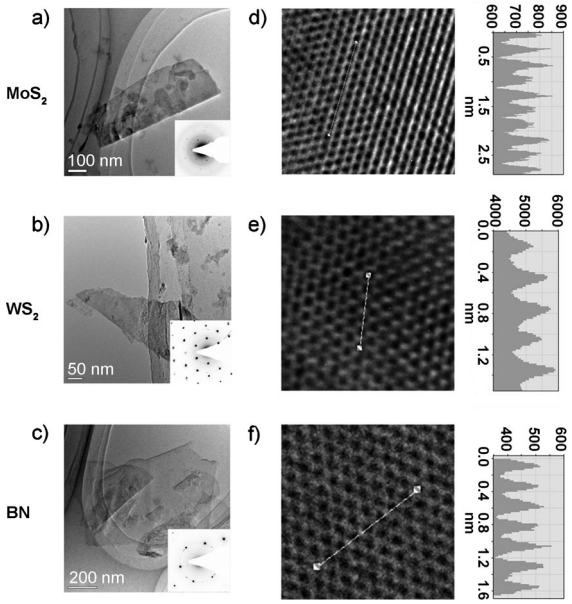


***Figure 2.*** HRTEM images of $MoS_2$ (a), $WS_2$ (b), and BN (c) nanosheets. The insets show the corresponding electron diffraction images. The scale bars are 100, 50, and 200 nm, respectively. d–f) Atomic-resolution HRTEM images.

Figure 1 d–f clearly show that the concentrations of the IGAs dispersions are strongly dependent on the volume fraction of ethanol in water. Such composition-dependent dispersion can be understood by the HSP theory, as different ethanol/water mixture have different $R_a$ values, which can be calculated by using Equations (1) and (2). Figure 1 reveals a strong correlation between the calculated $R_a$ and the dispersion concentration. As shown in Figure 1 d, when $MoS_2$ is dispersed in different solvents, the smallest calculated $R_a$ occurs for the 45 vol % ethanol/water mixture. Consistently, the experimental dispersion concentration in the 45 vol % mixed solvent is the highest. The highest concentration of $MoS_2$ in ethanol/water was estimated to be $0.018 \pm 0.003\ mg\,mL^{-1}$, which is approximately 13 times higher than that in pure ethanol and 68 times higher than that in pure water.

Similar to $MoS_2$, dispersion of $WS_2$ and BN also showed good consistency with the trend predicted by the HSP theory. In Figure 1 e, the dispersion of $WS_2$ reaches its maximum concentration in 35 vol % ethanol/water, and corresponds to a mass concentration of $0.032 \pm 0.003\ mg\,mL^{-1}$. Figure 1 f shows that the highest concentration of BN dispersion was obtained in 55 vol % ethanol/water with a mass concentration of $0.075 \pm 0.003\ mg\,mL^{-1}$, which is 37 times higher than that in isopropyl alcohol.[5]

The morphology of the IGAs obtained from the mixed-solvent exfoliation procedure was studied by TEM, which revealed that the majority of the nanomaterials are present as two-dimensional thin sheets in the dispersion. Figure 2 a–c confirm that the exfoliated nanomaterials exist as thin sheets with sizes varying from 100 nm to several micrometers. Folded edges with more than three layers were rarely observed, that is, the liquid-exfoliation process was highly efficient for obtaining few-layer sheets.[25–27] Besides, some fragments smaller than 50 nm were found to be adsorbed on the large sheets (Figure 2 a and c). High-resolution TEM (HRTEM) images (Figure 2 d–f) provide more detailed structural information.[5,18,28] The electron diffraction pattern indicated that the hexagonal lattices of the obtained IGAs were not damaged during the mixed-solvent exfoliation process. From atomic-resolution images, the lattice constants of $MoS_2$, $WS_2$, and BN were obtained to be 3.06, 3.13, and 2.42 Å, respectively, which are consistent with previously reported values.[19,29,30]

Atomic force microscopy (AFM) measurements indicated that the thickness of the $MoS_2$ sheets was around 2–4 nm (Figure 3 a). Given that the thickness of an $MoS_2$ monolayer is about 0.9–1.2 nm,[5] this suggests that the obtained $MoS_2$ sheets consist of 3–4 monolayers. Similarly, the thickness of $WS_2$ (ca. 3 nm, Figure 3 b) and BN (3–4 nm, Figure 3 c) sheets indicate that they also exist as few-layer nanosheets.

As colloidal particles often carry electrical charges in aqueous solution, zeta potentials of the samples were measured. The dispersed $MoS_2$, $WS_2$, and BN are all negatively charged, with zeta potentials of −20.7, −43.5, and −9.47 mV, respectively. The high surface charge ensures that the nanosheets repel each other in the dispersion, which explains their high stability. Owing to the high stability, volatile nature of the solvent, and the relatively high concentration, the dispersions are ideal for deposition of IGA thin films on various substrates by solution-processing methods, such as solution casting and filtration.[5]

Since the IGA nanosheets are negatively charged in the dispersions, electrophoretic deposition was used to deposit thin films of the nanosheets (Figure 4).[31] Figure 4 b shows that uniform thin films of the $MoS_2$, $WS_2$, and BN nanosheets

  

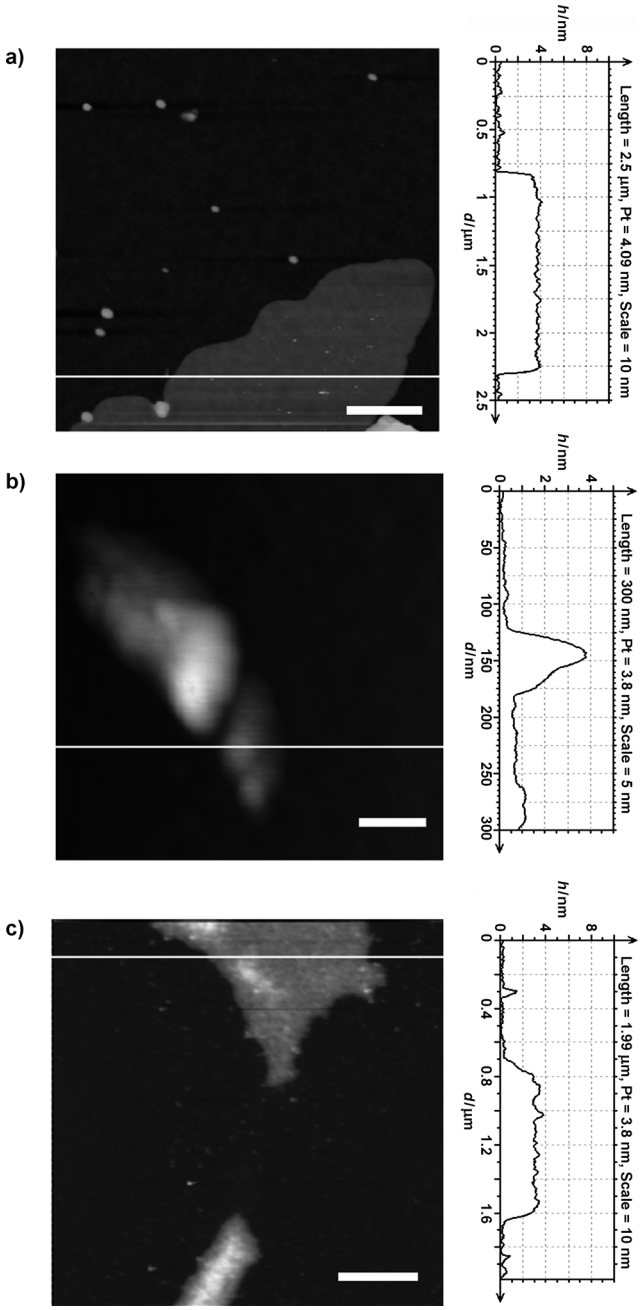


***Figure 3.*** Left: Representative AFM images of $MoS_2$ (a), $WS_2$ (b), and BN (c) nanosheets on mica. The scale bars are 500, 50, and 400 nm, respectively. Right: Height profiles along the white lines shown in the AFM images.

can be deposited onto various substrates, such as indium tin oxide (ITO) and Ti, under a dc field of 60 $V cm^{-1}$. SEM images (Figure 4c) confirm that the films consist of microscopic nanosheets uniformly deposited on the substrates. Electrophoretic deposition requires only a small amount of the dispersion, and the thicknesses of the films can be well controlled by means of the deposition time.

The thin films of IGAs prepared by electrophoretic deposition were tested for their photocurrent response (Figure 5). The thin films were irradiated with a 500 W Xe lamp and the photoconductivity response was recorded at a

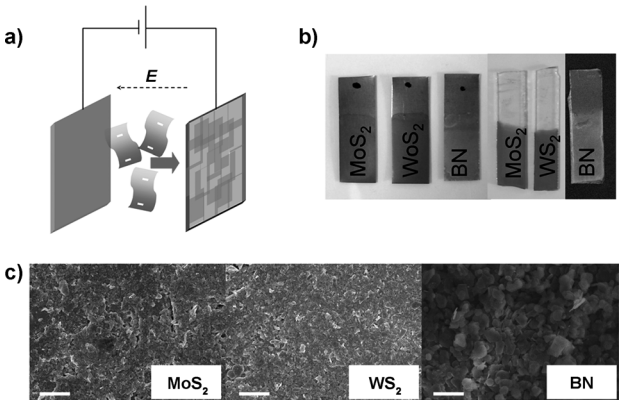


***Figure 4.*** a) Scheme of electrophoretic deposition. b) Photograph of deposited films on Ti and ITO substrates (60 $V cm^{-1}$ for 1 min). c) SEM images of $MoS_2$, $WS_2$, and BN nanosheets deposited on Ti substrate by electrophoresis. The scale bars are 2 μm.

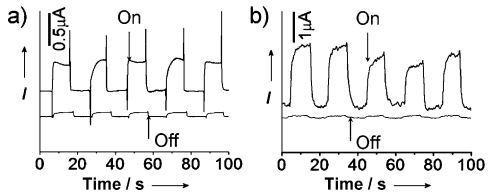


***Figure 5.*** Photocurrent response of the $MoS_2$ (a) and $WS_2$ (b) thin films (black curves) deposited on ITO by electrophoretic deposition. The response curves of their corresponding bulk materials are also shown for comparison (gray curves). The curves have been offset for clarity.

potential of 0.5 V. Both $MoS_2$ and $WS_2$ nanosheets showed a clear response to changing photointensity, and photocurrents of 0.42 and 1.92 μA, respectively, were found. Under the same conditions, spin-coated thin films of $MoS_2$ and $WS_2$ bulk powders gave current responses of only 0.07 and 0.08 μA, respectively. The thin film of BN sheets did not exhibit observable photocurrent response due to its large band gap. The dramatically enhanced photocurrent response can be attributed to the change from indirect to direct band structure when bulk $MoS_2$ and $WS_2$ are exfoliated into monolayer or few-layer nanosheets.[32,33]

As demonstrated above, two solvents previously thought to be "poor" can be combined into "good" solvents for exfoliating IGAs. This mixed-solvent method is versatile and scalable. Using low-boiling solvent mixtures to disperse IGAs offers several obvious advantages, including low cost, lower toxicity, freedom from additives, easy removal, and better biocompatibility.[26] Owing to the generic nature of the HSP theory, the mixed-solvent dispersion method can be regarded as a general approach toward the dispersion of various nanomaterials. As the number of possible solvent mixtures is virtually limitless, the mixed-solvent strategy effectively gives researchers great freedom in designing ideal solvent systems for each specific application. We anticipate that fast advances in areas like film formation, composite processing, and device fabrication involving layered IGAs will stem from these results.

  

### Experimental Section

All chemical reagents were of analytical grade and were obtained commercially. $MoS_2$, $WS_2$, or BN powder (30 mg, 1–6 μm, Aladdin Reagent Inc.) was added to 25 mL flasks. 10 mL of ethanol/water with EtOH volume fractions of 0 to 100 % was added as dispersion solvent. The sealed flask was sonicated for 8 h, and then the dispersion was centrifuged at 3000 rpm for 20 mins to remove aggregates. The supernatant was collected and UV/Vis spectra were measured to evaluate dispersion concentration.

Tapping-mode AFM (Agilent SPM 5500), HRTEM (Tecnai-G2-F30), and field-emission SEM (Hitachi S4800) were used to study the morphology of the nanomaterials. Zeta potentials were collected by a Nano ZS 3600 (Malvern Instruments Ltd.).

Received: July 29, 2011
Published online: September 27, 2011

**Keywords:** inorganic graphene analogues · layered compounds · nanostructures · solvent effects · thin films

[1] A. K. Geim, K. S. Novoselov, *Nat. Mater.* **2007**, *6*, 183 – 191.
[2] X. Huang, Z. Yin, S. Wu, X. Qi, Q. He, Q. Zhang, Q. Yan, F. Boey, H. Zhang, *Small* **2011**, *7*, 1876 – 1902.
[3] X. Huang, X. Qi, F. Boey, H. Zhang, *Chem. Soc. Rev.* **2011**, DOI: 10.1039/C1CS15078B.
[4] H. Jiang, *Small* **2011**, *7*, 2413 – 2427.
[5] J. N. Coleman, M. Lotya, A. O'Neill, S. D. Bergin, P. J. King, U. Khan, K. Young, A. Gaucher, S. De, R. J. Smith, I. V. Shvets, S. K. Arora, G. Stanton, H.-Y. Kim, K. Lee, G. T. Kim, G. S. Duesberg, T. Hallam, J. J. Boland, J. J. Wang, J. F. Donegan, J. C. Grunlan, G. Moriarty, A. Shmeliov, R. J. Nicholls, J. M. Perkins, E. M. Grieveson, K. Theuwissen, D. W. McComb, P. D. Nellist, V. Nicolosi, *Science* **2011**, *331*, 568 – 571.
[6] C. N. R. Rao, A. Nag, *Eur. J. Inorg. Chem.* **2010**, 4244 – 4250.
[7] K. S. Novoselov, D. Jiang, F. Schedin, T. J. Booth, V. V. Khotkevich, S. V. Morozov, A. K. Geim, *Proc. Natl. Acad. Sci. USA* **2005**, *102*, 10451 – 10453.
[8] D. Golberg, Y. Bando, Y. Huang, T. Terao, M. Mitome, C. Tang, C. Zhi, *ACS Nano* **2010**, *4*, 2979 – 2993.
[9] B. Radisavljevic, A. Radenovic, J. Brivio, V. Giacometti, A. Kis, *Nat. Nanotechnol.* **2011**, *6*, 147 – 150.
[10] H. Zeng, C. Zhi, Z. Zhang, X. Wei, X. Wang, W. Guo, Y. Bando, D. Golberg, *Nano Lett.* **2010**, *10*, 5049 – 5055.
[11] W. J. Yu, S. Y. Lee, S. H. Chae, D. Perello, G. H. Han, M. Yun, Y. H. Lee, *Nano Lett.* **2011**, *11*, 1344 – 1350.
[12] S. Yin, Y. Zhang, J. Kong, C. Zou, C. M. Li, X. Lu, J. Ma, F. Y. C. Boey, X. Chen, *ACS Nano* **2011**, *5*, 3831 – 3838.
[13] K. Chang, W. Chen, *ACS Nano* **2011**, *5*, 4720 – 4728.
[14] C. Y. Zhi, Y. Bando, C. C. Tang, H. Kuwahara, D. Golberg, *Adv. Mater.* **2009**, *21*, 2889 – 2893.
[15] G. Wang, X.-G. Zhu, Y.-Y. Sun, Y.-Y. Li, T. Zhang, J. Wen, X. Chen, K. He, L.-L. Wang, X.-C. Ma, J.-F. Jia, S. B. Zhang, Q.-K. Xue, *Adv. Mater.* **2011**, *23*, 2929 – 2932.
[16] L. Xie, X. Ling, Y. Fang, J. Zhang, Z. Liu, *J. Am. Chem. Soc.* **2009**, *131*, 9890 – 9891.
[17] R. V. Gorbachev, I. Riaz, R. R. Nair, R. Jalil, L. Britnell, B. D. Belle, E. W. Hill, K. S. Novoselov, K. Watanabe, T. Taniguchi, A. K. Geim, P. Blake, *Small* **2011**, *7*, 465 – 468.
[18] H. S. S. Ramakrishna Matte, A. Gomathi, A. K. Manna, D. J. Late, R. Datta, S. K. Pati, C. N. R. Rao, *Angew. Chem.* **2010**, *122*, 4153 – 4156; *Angew. Chem. Int. Ed.* **2010**, *49*, 4059 – 4062.
[19] A. Nag, K. Raidongia, K. P. S. S. Hembram, R. Datta, U. V. Waghmare, C. N. R. Rao, *ACS Nano* **2010**, *4*, 1539 – 1544.
[20] M. Lotya, Y. Hernandez, P. J. King, R. J. Smith, V. Nicolosi, L. S. Karlsson, F. M. Blighe, S. De, Z. Wang, I. T. McGovern, G. S. Duesberg, J. N. Coleman, *J. Am. Chem. Soc.* **2009**, *131*, 3611 – 3620.
[21] A. O'Neill, U. Khan, P. N. Nirmalraj, J. Boland, J. N. Coleman, *J. Phys. Chem. C* **2011**, *115*, 5422 – 5428.
[22] Y. Hernandez, V. Nicolosi, M. Lotya, F. M. Blighe, Z. Sun, S. De, I. T. McGovern, B. Holland, M. Byrne, Y. K. Gun'Ko, J. J. Boland, P. Niraj, G. Duesberg, S. Krishnamurthy, R. Goodhue, J. Hutchison, V. Scardaci, A. C. Ferrari, J. N. Coleman, *Nat. Nanotechnol.* **2008**, *3*, 563 – 568.
[23] C. M. Hansen, *Hansen Solubility Parameters: A User's Handbook*, CRC, Boca Raton, **2007**.
[24] J. N. Coleman, *Adv. Funct. Mater.* **2009**, *19*, 3680 – 3695.
[25] L. Song, L. Ci, H. Lu, P. B. Sorokin, C. Jin, J. Ni, A. G. Kvashnin, D. G. Kvashnin, J. Lou, B. I. Yakobson, P. M. Ajayan, *Nano Lett.* **2010**, *10*, 3209 – 3215.
[26] Y. Lin, T. V. Williams, T.-B. Xu, W. Cao, H. E. Elsayed-Ali, J. W. Connell, *J. Phys. Chem. C* **2011**, *115*, 2679 – 2685.
[27] J. H. Warner, M. H. Rummeli, A. Bachmatiuk, B. Buchner, *ACS Nano* **2010**, *4*, 1299 – 1304.
[28] J. H. Warner, M. H. Rummeli, T. Gemming, B. Buchner, G. A. D. Briggs, *Nano Lett.* **2008**, *9*, 102 – 106.
[29] S. Lebègue, O. Eriksson, *Phys. Rev. B* **2009**, *79*, 115409.
[30] A. Klein, S. Tiefenbacher, V. Eyert, C. Pettenkofer, W. Jaegermann, *Thin Solid Films* **2000**, *380*, 221 – 223.
[31] S. J. An, Y. Zhu, S. H. Lee, M. D. Stoller, T. Emilsson, S. Park, A. Velamakanni, J. An, R. S. Ruoff, *J. Phys. Chem. Lett.* **2010**, *1*, 1259 – 1263.
[32] J. C. McMenamin, W. E. Spicer, *Phys. Rev. B* **1977**, *16*, 5474.
[33] A. Kuc, N. Zibouche, T. Heine, *Phys. Rev. B* **2011**, *83*, 245213.

  